Clim. Past, 14, 1015–1033, 2018
https://doi.org/10.5194/cp-14-1015-2018

Climate of the Past
Open Access
EGU

Paleoceanography and ice sheet variability offshore Wilkes Land, Antarctica – Part 2: Insights from Oligocene–Miocene dinoflagellate cyst assemblages

Peter K. Bijl[1,*], Alexander J. P. Houben[2], Julian D. Hartman[1], Jörg Pross[3], Ariadna Salabarnada[4], Carlota Escutia[4], and Francesca Sangiorgi[1]

[1]Marine Palynology and Paleoceanography, Laboratory of Palaeobotany and Palynology, Department of Earth Sciences, Faculty of Geosciences, Utrecht University. P.O. Box 80.115, 3508 TC Utrecht, the Netherlands
[2]Geological Survey of the Netherlands, Netherlands Organisation for Applied Scientific Research (TNO), Princetonlaan 6, 3584 CB, Utrecht, the Netherlands
[3]Paleoenvironmental Dynamics Group, Institute of Earth Sciences, Heidelberg University, Im Neuenheimer Feld 234, 69120 Heidelberg, Germany
[4]Instituto Andaluz de Ciencias de la Tierra, CSIC-UGR, 18100 Armilla, Spain
[*]Invited contribution by Peter K. Bijl, recipient of the EGU Arne Richter Award for Outstanding Early Career Scientists 2014.

Correspondence: Peter K. Bijl (p.k.bijl@uu.nl)

Received: 13 November 2017 – Discussion started: 5 December 2017
Revised: 9 May 2018 – Accepted: 21 June 2018 – Published: 11 July 2018

Abstract. Next to atmospheric CO_2 concentrations, ice-proximal oceanographic conditions are a critical factor for the stability of Antarctic marine-terminating ice sheets. The Oligocene and Miocene epochs (~ 34–5 Myr ago) were time intervals with atmospheric CO_2 concentrations between those of present-day and those expected for the near future. As such, these past analogues may provide insights into ice-sheet volume stability under warmer-than-present-day climates. We present organic-walled dinoflagellate cyst (dinocyst) assemblages from chronostratigraphically well-constrained Oligocene to mid-Miocene sediments from Integrated Ocean Drilling Program (IODP) Site U1356. Situated offshore the Wilkes Land continental margin, East Antarctica, the sediments from Site U1356 have archived the dynamics of an ice sheet that is today mostly grounded below sea level. We interpret dinocyst assemblages in terms of paleoceanographic change on different timescales, i.e. with regard to both glacial–interglacial and long-term variability. Our record shows that a sea-ice-related dinocyst species, *Selenopemphix antarctica*, occurs only for the first 1.5 Myr of the early Oligocene, following the onset of full continental glaciation on Antarctica, and after the Mid-Miocene Climatic Optimum. Dinocysts suggest a weaker-than-modern sea-ice season for the remainder of the Oligocene and Miocene. The assemblages generally bear strong similarity to present-day open-ocean, high-nutrient settings north of the sea-ice edge, with episodic dominance of temperate species similar to those found in the present-day subtropical front. Oligotrophic and temperate surface waters prevailed over the site notably during interglacial times, suggesting that the positions of the (subpolar) oceanic frontal systems have varied in concordance with Oligocene–Miocene glacial–interglacial climate variability.

1 Introduction

The proportion of the East Antarctic ice sheet that is presently grounded below sea level is much larger than originally interpreted (Fretwell et al., 2013). This implies that a larger part of the continental ice sheet is sensitive to basal melting by warm waters than previously thought (Shepherd et al., 2012; Rignot et al., 2013; Wouters et al., 2015), and that a higher amplitude and faster rate of sea-level rise is to be expected under future climate warming than previously acknowledged (IPCC, 2013). Studying the amount of and variability in Antarctic ice volume in periods with high atmospheric CO_2 concentrations (pCO_2) provides addi-

tional insight into ice–ocean feedback processes. Foster and Rohling (2013) compared sea-level and atmospheric pCO_2 concentrations on geological timescales. Their study suggests that global ice sheets were rather insensitive to climate change when atmospheric pCO_2 ranged between 400 and 650 parts per million in volume (ppmv). During the Oligocene and Miocene, atmospheric pCO_2 ranged between 400 and 650 ppmv (Foster et al., 2012; Badger et al., 2013; Greenop et al., 2014). Crucially, similar pCO_2 levels are expected for the near future given unabated carbon emissions (IPCC, 2013), implying that global ice volume may not change much under these pCO_2 scenarios.

In contrast to the invariant global ice volume inferred by Foster and Rohling (2013), a strong (up to 1 per mille, ‰) variability is preserved in deep-sea benthic foraminiferal oxygen isotope (hereafter benthic $\delta^{18}O$) data (e.g. Pälike et al., 2006b; Beddow et al., 2016; Holbourn et al., 2007; Liebrand et al., 2011, 2017; De Vleeschouwer et al., 2017). These benthic $\delta^{18}O$ data reflect changes in continental ice volume (primarily on Antarctica) and deep-sea temperature. The latter is strongly coupled to polar surface water temperature, as deep-water formation was predominantly at high latitudes at that time (Herold et al., 2011). High-amplitude variations in benthic $\delta^{18}O$ thus suggest either (i) strong climate dynamics in the high latitudes with relatively minor ice volume change (which would be in accordance with numerical modelling experiments (Barker et al., 1999) and the interpretation of Foster and Rohling, 2013), or (ii) strong fluctuations in Antarctic ice volume, with relatively subdued temperature variability (which would be in accordance with indications for unstable Antarctic ice sheets under warmer-than-present climates (Cook et al., 2013; Greenop et al., 2014; Rovere et al., 2014; Sangiorgi et al., 2018). If one assumes a present-day $\delta^{18}O$ composition (−42 ‰ versus standard mean ocean water) for Oligocene–Miocene Antarctic ice sheets and modern deep-water temperature (2.5 °C), the benthic $\delta^{18}O$ fluctuations during the Oligocene–Miocene suggest long-term ice-sheet variability to have fluctuated considerably (Liebrand et al., 2017). Similarly strong fluctuations were observed in sedimentary records from the Gippsland Basin, southeast Australia (Gallagher et al., 2013). Meanwhile, deep-sea temperatures have fluctuated considerably as well during the Oligocene and Miocene (Lear et al., 2004), which is further evident from ice-free geologic episodes (Zachos et al., 2008). Therefore, a combination of deep-sea temperature and ice volume changes is likely represented in these records. Further ice-proximal reconstructions of climate, ice-sheet and oceanographic conditions are required to provide an independent assessment of the stability of ice sheets under these higher-than-present-day pCO_2 concentrations.

While Oligocene–Miocene climates may bear analogy to our future in terms of pCO_2 concentrations, the uncertainties and differences in Antarctic paleotopography must be considered in any such comparison, as this factor critically determines the proportion of marine-based versus land-based ice. An Antarctic continent with low topography would result in more ice sheets being potentially sensitive to basal melt and as such a higher sensitivity of these ice sheets to climate change. Moreover, the fundamentally different paleogeographic configuration of the Southern Ocean during that time compared to today should also be considered (Fig. 1). The development and strength of the Antarctic Circumpolar Current (ACC) connecting the Atlantic, Indian and Pacific ocean basins (Barker and Thomas, 2004; Olbers et al., 2004) depend on the basin configuration (i.e. the width and depth of the gateways as well as the position of the land masses). The exact timing when the ACC reached its modern-day strength is still uncertain, ranging from the middle Eocene (41 Ma) to as young as Miocene (23 Ma; Scher and Martin, 2004; Hill et al., 2013; Scher et al., 2015). Whether and, if so, how the development of the ACC has influenced latitudinal heat transport, ice–ocean interactions and the stability of Antarctic continental ice has remained poorly understood.

To directly assess the role of ice-proximal oceanography on ice-sheet stability during the Oligocene–Miocene, ice-proximal proxy records are required. Several ocean drilling expeditions have been undertaken in the past to provide insight into the history of the Antarctic ice sheets (Barrett, 1989; Wise and Schlich, 1992; Barker et al., 1998; Robert et al., 1998; Wilson et al., 2000; Cooper and O'Brien, 2004; Exon et al., 2004; Harwood et al., 2006; Escutia and Brinkhuis, 2014). For some of the retrieved sedimentary archives, age control was particularly challenging due to the paucity of useful means to calibrate them to the international timescale. As a consequence, the full use of these archives for the generation of paleoceanographic proxy records and ice-sheet reconstructions has remained limited.

In 2010, Integrated Ocean Drilling Program (IODP) Expedition 318 drilled an inshore-to-offshore transect off Wilkes Land (Fig. 1a), a sector of East Antarctica that is interpreted to be highly sensitive to continental ice-sheet melt (Escutia et al., 2011). The sediments recovered from IODP Site U1356 are from the continental rise of this margin (Escutia et al., 2011) and hence contain a mixture of shelf-derived material and pelagic sedimentation. Dinocyst events in this record have been recently tied to the international timescale through integration with calcareous nannofossil, diatom and magnetostratigraphic data (Bijl et al., 2018a). By Southern Ocean standards, the resulting stratigraphic age frame for the Oligocene–Miocene record of Site U1356 (Fig. 2; Table 1) is of high resolution. In this paper, we investigate the dinocyst assemblages from this succession by utilising the strong relationships between dinocyst assemblage composition and surface water conditions of today's Southern Ocean (Prebble et al., 2013). We reconstruct the oceanographic regimes during the Oligocene and mid-Miocene and evaluate their implications. We further compare the palynological data with lithological observations and their interpretations from Salabarnada et al. (2018). Pairing the sedimentological interpretations and biomarker-derived absolute sea-surface tem-

Table 1. Age constraints for the Oligocene–Miocene of Hole U1356A.

Type	FO/LO	Genus, chron	Age (Gradstein et al., 2012)	Top core	Top interval	Bottom core	Bottom interval	Depth average	Error
CONOP			10.76					98.66	
CONOP			10.92					133.80	
CONOP			13.41					133.81	
PM	(o)	C5ACn	14.07	22R-2,	75	22R-2,	90	203.23	0.07
PM	(y)	C5Bn.2n	15.03	30R-2,	50	30R-2,	75	279.63	0.13
PM	(o)	C5Cn.1n	16.27	39R-1,	35	39R-1,	65	364.10	0.15
PM	(o)	C5Cn.3n	16.72	42R-2,	59	43R-1,	25	398.28	3.98
			17.50	44R-CC		45R-CC		416.90	
			23.00	44R-CC		45R-CC		416.91	
PM	(o)	C6Cn.2n	23.03	45R-CC	40	46R-1	65	426.78	5.00
PM	(o)	C6Cn.3n	23.30	50R-1,	0			469.00	9.00
PM	(y)	C7An	24.76	63R-3,	85	63R-3,	120	597.12	0.17
PM	(o)	C7An	24.98	64R-1,	130	64R-1,	135	604.33	0.02
PM	(o)	C8n.1n	25.26	68R-2,	20	68R-2,	75	643.38	0.27
PM	(y)	C8n.2n	25.30	69R-2,	20	69R-2,	25	652.58	0.02
PM	(o)	C8n.2n	25.99	71R-6,	115	72R-1,	10	678.98	0.92
PM	(y)	C9n	26.42	73R-4,	90	75R-1,	15	701.66	7.09
PM	(o)	C9n	27.44	76R-6,	35	76R-6,	40	725.09	0.02
PM	(o)	C11n.2n	29.97	82R-6,	35	82R-6,	40	782.68	0.03
PM	(y)	C13n	33.16	93R-1,117		93R-2,	28	878.00	0.23

perature (SST) reconstructions from Site U1356 (Hartman et al., 2017) with our dinocyst assemblage data, we reconstruct the paleoceanographic conditions off Wilkes Land and assess their variability on both glacial–interglacial and longer-term timescales.

2 Material

2.1 Site description for IODP Hole U1356A

Samples were taken from IODP Hole U1356A, the only hole from Site U1356, cored on the continental rise of the Wilkes Land margin, East Antarctica (Fig. 1a; present coordinates 63°18.6′ S, 135°59.9′ E; Escutia et al., 2011). The paleolatitude calculator of van Hinsbergen et al. (2015) was used to reconstruct the paleolatitudinal history of the site (Fig. 1, between -59.8 ± 4.8 and $-61.5 \pm 3.3°$ S between 34 and 13 Ma, respectively). Hole U1356A reaches a depth of 1006.4 m into the seabed (Escutia et al., 2011). Oligocene to upper Miocene sediments were recovered between 890 and 3 m b.s.f. (metres below sea floor, Fig. 2; Tauxe et al., 2012; revised according to Bijl et al., 2018a). The uppermost 95 m of the hole was poorly recovered; sediments consisted of unconsolidated mud strongly disturbed by rotary drilling (Escutia et al., 2011). Hence, we focused our investigation on the interval between Cores 11R and 95R Section 3 (95.4–894 m b.s.f.; 10.8–33.6 Ma; Fig. 2).

2.2 Lithology in IODP Hole U1356A

In the interval between 95.4 and 894 m b.s.f., nine lithologic units have been recognised during shipboard analysis (Fig. 2; Escutia et al., 2011). Salabarnada et al. (2018) present a detailed lithologic column of the Oligocene and Miocene sediments. The lithologic facies described in Salabarnada et al. (2018) will help us compare paleoceanographic differences among climatic extremes. Salabarnada et al. (2018) distinguished various lithologies along with interpretations of their depositional settings which can be summarised as (1) laminated silty clay sediments (interpreted as glacial deposits; hereafter Fg), (2) bioturbated siltstones and claystones that in some intervals are carbonate cemented (interpreted as interglacial deposits, hereafter Fi), and (3) perturbed mass transport deposits (MTDs): slumps and debris flows. We refer to Salabarnada et al. (2018; Fig. S2 in their Supplement) for a detailed description of these facies, and to the supplementary datasets on PANGAEA (Bijl et al., 2018b) for more detailed separation of our palynological results per facies type.

2.3 Bio-magnetostratigraphic age model for IODP Hole U1356A

Stratigraphic constraints for the Oligocene–Miocene succession from IODP Hole U1356A are provided through calcareous nanoplankton, radiolarian, diatom and sparse palynological biostratigraphy, complemented by magnetostratigraphy (Tauxe et al., 2012). Bijl et al. (2018a) and Cramp-

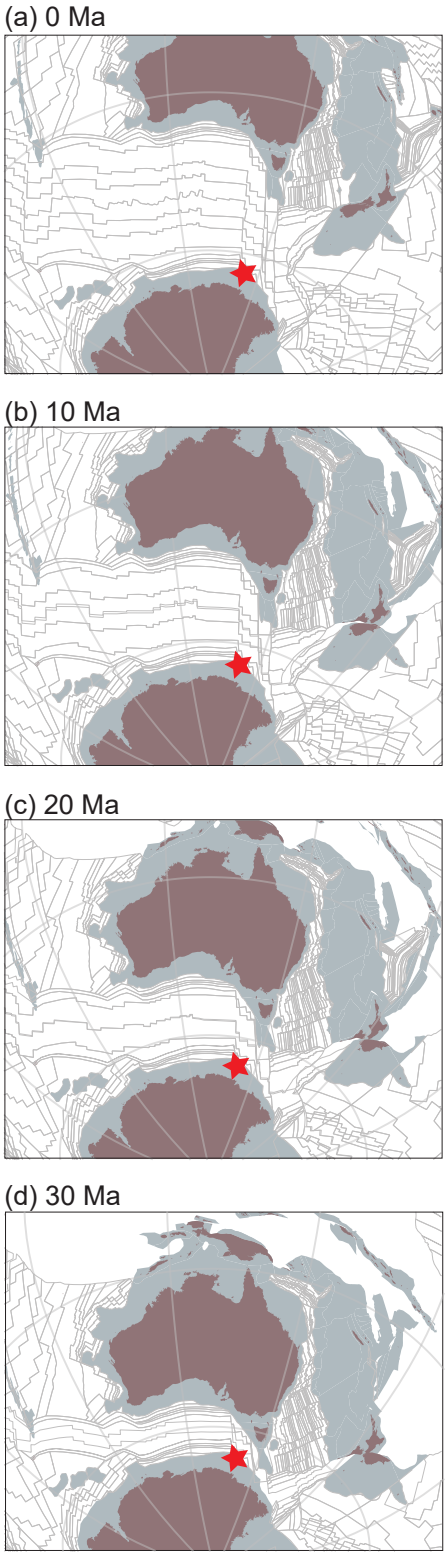

Figure 1. Paleogeography of the southwestern Pacific Ocean and position of IODP Site U1356 (red star) at **(a)** 0 Ma, **(b)** 10 Ma, **(c)** 20 Ma and **(d)** 30 Ma. Figures are modified after Bijl et al. (2018a). Reconstructions were adapted from G plates, with the plate circuit from Seton et al. (2012) and absolute plate positions of Torsvik et al. (2012).

ton et al. (2016) have updated the existing age model for Site U1356 for the Oligocene and Miocene parts of the succession, respectively. In their efforts, they recalibrated the tie points to the international timescale of Gradstein et al. (2012). We here follow their revision of the age model (Table 1). We infer ages by linear interpolation among tie points (Fig. 2; Table 1).

2.4 Depositional setting at IODP Site U1356

The depositional setting at Site U1356 changed from a shallow mid-continental shelf in the early Eocene (Bijl et al., 2013a) to a deep continental rise environment by the Oligocene (Houben et al., 2013) due to subsidence of the Wilkes Land margin (e.g. Close et al., 2009). Regional correlation of the facies at Hole U1356A via seismic profiles suggests a mix of distal-submarine fan and hemipelagic sedimentation during the early Oligocene, grading into channel–levee deposits in the later Oligocene (Escutia et al., 2011). The boundary between these two different depositional settings is at ∼ 650 m b.s.f.; there, sedimentation rates increase, and the documentation of mass-transport deposits from this depth upwards suggests shelf-derived erosion events on the Wilkes Land continental slope (Escutia et al., 2011).

3 Methods

3.1 Palynological sample processing

The sample processing and analytical protocols as followed in this study are in accordance with standard procedures and have been previously described by Bijl et al. (2013b, 2018a). The 25 species of dinocysts new to science, which are formally (two species) and informally (23 species) described in Bijl et al. (2018a), fit into known and extant genera, and therefore could be confidently included in the ecological groups as described below. We refer to Bijl et al. (2018a) for an extensive overview (including plates) of the dinocyst species encountered.

3.2 Ecological grouping of dinocyst taxa

Bijl et al. (2018a) provided additional statistical evidence to distinguish in situ dinocysts from those that are reworked from older strata. In this paper, we follow the interpretations of Bijl et al. (2018a) and divide the dinocyst species into a reworked and an in situ group (Table 2). To use the in situ dinocyst assemblages for oceanographic reconstructions, we rely on the observation that many taxa in the fossil assemblages have morphologically closely related modern counterparts. This approach takes advantage of studies on the present-day relationship between Southern Ocean microplankton in general and dinoflagellate cysts in particular and their surface water characteristics (e.g. Eynaud et al., 1999; Esper and Zonneveld, 2002, 2007; Prebble et

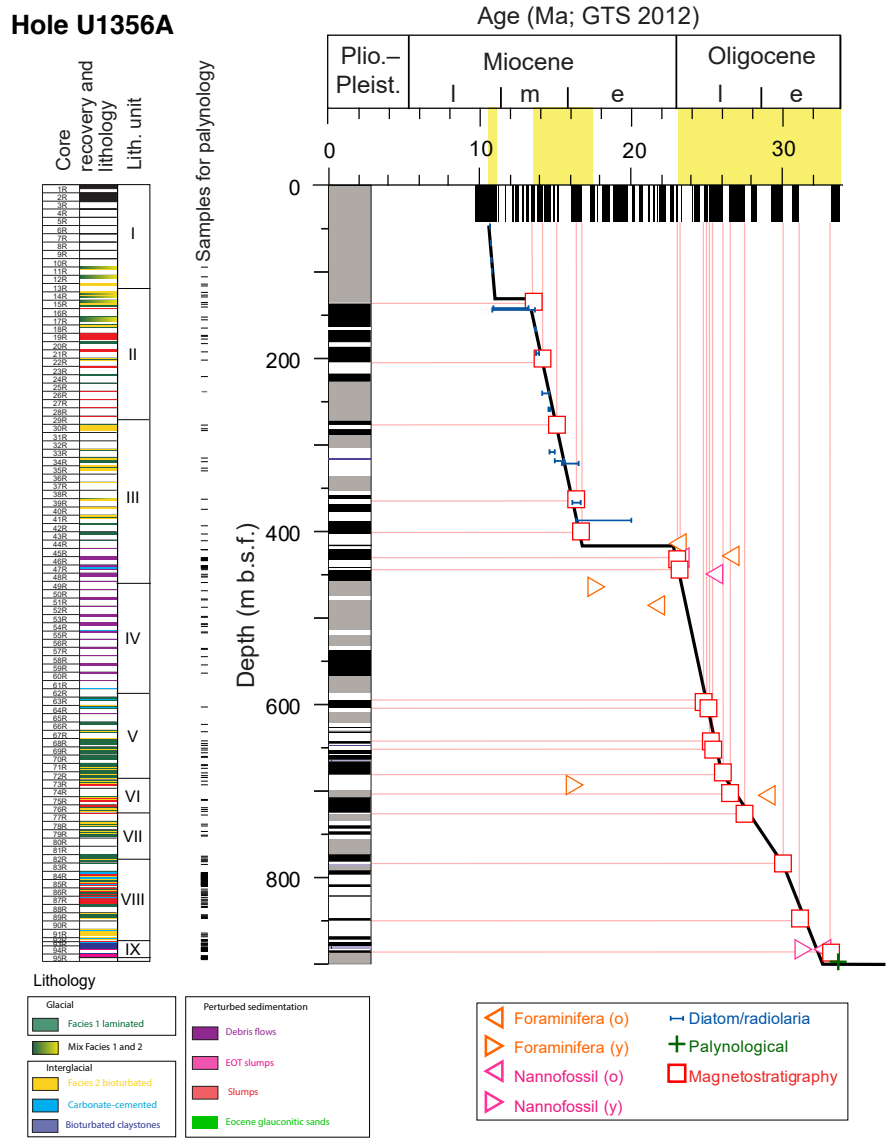

Figure 2. Age model for the Oligocene–Miocene interval of Hole U1356A. Core recovery, lithostratigraphic facies after Salabarnada et al. (2018; see also Sangiorgi et al., 2018) and lithostratigraphic units (Escutia et al., 2011). Samples taken for palynology and age–depth plot (tie points were derived from Tauxe et al., 2012, which has been recalibrated to the GTS2012 timescale of Gradstein et al., 2012, and modified based on Crampton et al., 2016). Grey intervals in paleomagnetic data reflect unknown paleomagnetic orientation, either due to absence of core recovery or poor signal. (o): old end; (y): young end. Figure modified from Bijl et al. (2018a).

al., 2013). We assign Oligocene–Miocene dinocyst taxa to present-day eco-groups interpreted from the clusters identified by Prebble et al. (2013), which appear to be closely related to the oceanic frontal systems in the Southern Ocean (Fig. 3). Supporting evidence for the ecologic affinities of the dinocyst groups comes from empirical data, such as correlation of abundances with other sediment properties or proxies (Sluijs et al., 2005; Egger et al., 2018), for instance with regard to the affinities of *Nematosphaeropsis labyrinthus*, *Operculodinium* spp., *Pyxidinopsis* cpx. (this includes *Corrudinium* spp. and *Cerebrocysta* spp.) and *Impagidinium* spp. There is further abundant evidence, both empirically (e.g. Sluijs et al., 2003; Houben et al., 2013) and from modern observations (Zonneveld et al., 2013; Prebble et al., 2013; Eynaud et al., 1999), that links the abundance of protoperidinioid dinocysts to high surface water productivity. The arguably most important inference from the surface-sediment sample study of Prebble et al. (2013) is that *Selenopemphix antarctica* is common to dominant (10–90 %) south of the Antarctic polar front (AAPF). In particular, the Antarctic continental shelf exhibits a consistently high relative abundance of *Selenopemphix antarctica*. In addition to the sur-

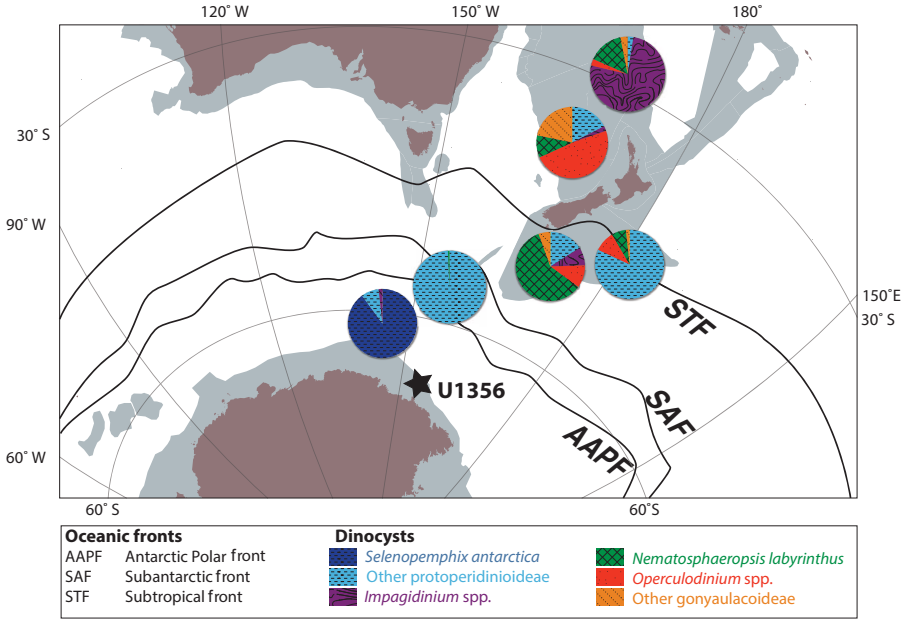

Figure 3. Generic representation of present-day distributions of dinocysts in surface sediments in the Southern Ocean. The dinocyst pie charts represent average dinocyst assemblage compositions for surface sediments underneath oceanic frontal zones in the Southern Ocean. Figure modified from Sangiorgi et al. (2018); data replotted from Prebble et al. (2013).

face samples of Prebble et al. (2013), this is also evident at the Wilkes Land margin proper (IODP Site U1357; Julian D. Hartman, Peter K. Bijl, and Francesca Sangiorgi, personal observation), at Prydz Bay (Storkey, 2006), in the Weddell (Harland and Pudsey, 1999) and Ross seas (Julian D. Hartman, Peter K. Bijl, and Francesca Sangiorgi, personal observation), and in the southern Indian Ocean (Marret and De Vernal, 1997): samples all contain very abundant to dominant (> 50 to 90 %) *S. antarctica*. The dominance of this species becomes even stronger when considering that assemblages in these surface samples often include cysts that are not easily preserved in older sediments such as that of *Polarella glacialis*. Leaving these dinocysts out of the dinocyst sum increases the relative abundance of *Selenopemphix antarctica* in surface samples. Notably, surface-sediment samples outside of the AAPF never have dominant (∼ 90 %) *Selenopemphix antarctica* (Prebble et al., 2013). Another important observation is that the surface-sediment samples south of the AAPF are generally devoid of gonyaulacean dinocysts, with the exception of two species of *Impagidinium* (i.e. *I. pallidum* and *I. sphaericum*) that may occur, although neither abundantly (Prebble et al., 2013) nor exclusively (e.g. Zevenboom, 1995; Zonneveld et al., 2013), in ice-proximal locations. Abundant *Nematosphaeropsis labyrinthus* occurs exclusively in regions outside of the subantarctic front, and particularly near the subtropical front. Thus, we conclude from the available literature a dominance of *S. antarctica* south of the AAPF, a dominance of other protoperidinioid dinocysts at and north of the AAPF, mixed protoperidinioid and gonyaulacoid dinocysts (with a notable occurrence of *Nematosphaeropsis labyrinthus* at the subantarctic front, and mixed gonyaulacoid dinocysts at and outside of the subtropical front. These trends represent a north–south transition from sea-ice-influenced conditions to cold-upwelling, high-nutrient conditions to warm-temperate, lower-nutrient conditions. We use these affinities to reconstruct past oceanographic conditions at the Wilkes Land continental margin.

4 Results

4.1 Palynological groups

In our palynological analysis we separated palynomorph groups into four categories: reworked dinocysts (following Bijl et al., 2018a; Table 2), in situ dinocysts, acritarchs and terrestrial palynomorphs. Our palynological slides further contain a varying amount of pyritised diatoms and a minor component of amorphous organic matter, which is not further considered in this study. The relative and absolute abundances of the four palynomorph groups vary considerably throughout the studied interval (Fig. 4). Reworked dinocysts are ubiquitous throughout the record, and are particularly abundant in the lowermost 40 m of the Oligocene and in the upper Oligocene. In situ dinocysts dominate mid-Oligocene and mid-Miocene palynomorph assemblages. Chorate, sphaeromorph and *Cymatiosphaera*-like acritarchs (which are not further taxonomically subdivided) dominate the assemblage in the upper Oligocene and into the mid-Miocene, while terrestrial palynomorphs (which are consid-

Table 2. List of assumed in situ and reworked dinoflagellate cyst taxa encountered in this study. See Bijl et al. (2018a) for informal species descriptions and discussion about which species are considered reworked and in situ.

In situ taxa	Reworked taxa
Adnatosphaeridium? sp.	*Achilleodinium biformoides*
Ataxodinium choane	*Achomosphaera alcicornu*
Batiacasphaera compta	*Aiora fenestrata*
Batiacasphaera spp. (pars.)	*Aireiana verrucosa*
Batiacasphaera hirsuta	*Adnatosphaeridium* spp.
Batiacasphaera micropapillata	*Alisocysta circumtabulata*
Batiacasphaera minuta	*Alterbidinium distinctum*
Batiacasphaera sphaerica	*Apectodinium* spp.
Batiacasphaera sp. A	*Arachnodinium antarcticum*
Batiacasphaera sp. B	*Areoligera* spp. (pars)
Batiacasphaera sp. C	*Areoligera semicirculata*
Batiacasphaera sp. D	*Cerebrocysta bartonensis*
Brigantedinium simplex	*Charlesdowniea clathrata*
Brigantedinium pynei	*Charlesdowniea edwardsii*
Brigantedinium sp. A	*Cooksonidinium capricornum*
Brigantedinium sp. B	*Cordosphaeridium fibrospinosum*
Brigantedinium sp. C	*Cordosphaeridium furniculatum*
Brigantedinium sp. D	*Corrudinium incompositum*
Cerebrocysta WR small	*Corrudinium regulare*
Cerebrocysta delicata	*Cribroperidinium* spp.
Cerebrocysta sp. A	*Damassadinium crassimuratum*
Cleistosphaeridium sp. B	*Dapsilidinium* spp.
Cleistosphaeridium sp. A	*Deflandrea* sp. A sensu Brinkhuis et al. (2003a, b)
Cordosphaeridium minutum	*Deflandrea antarctica*
Corrudinium labradori	*Deflandrea cygniformis*
Corrudinium sp. A	*Diphyes colligerum*
Cryodinium? sp.	*Deflandrea* spp. indet
Distatodinium spp.	*Eisenackia circumtabulata*
Edwardsiella sexispinosa	*Enneadocysta diktyostila*
Elytrocysta sp. A	*Enneadocysta multicornuta*
Elytrocysta brevis	*Eocladopyxis tessellata*
Gelatia inflata	*Fibrocysta axialis*
Habibacysta? spp.	*Glaphyrocysta intricata*
Homotryblium spp.	*Glaphyrocysta pastielsii*
Hystrichokolpoma bullatum	*Heteraulacacysta leptalea*
Huystrichosphaeropsis obscura	*Histiocysta palla*
Impagidinium spp. (pars)	*Hystrichokolpoma pusilla*
Impagidinium aculeatum	*Hystrichokolpoma rigaudiae*
Impagidinium cantabrigiense	*Hystrichokolpoma truncatum*
Impagidinium elegans	*Hystrichosphaeridium truswelliae*
Impagidinium elongatum	*Hystrichosphaeridium tubiferum*
Impagidinium pacificum	*Impagidinium maculatum*
Impagidinium pallidum	*Impagidinium waipawense*
Impagidinium paradoxum	*Kenleyia* spp.
Impagidinium patulum	*Manumiella druggii*
Impagidinium plicatum	*Melitasphaeridium pseudorecurvatum*
Impagidinium velorum	*Membranophoridium perforatum*
Impagidinium victorianum	*Octodinium askiniae*
Impagidinium sp. A	*Odontochitin*a spp.
Impagidinium sphaericum	*Operculodinium* spp.
Invertocysta tabulata	*Phthanoperidinium antarcticum*
Islandinium spp.	*Phthanoperidinium stockmansii*
Lejeunecysta attenuata	*Polysphaeridium* spp.
Lejeunecysta adeliense	*Rhombodinium* sp.
Lejeunecysta fallax	*Schematophora speciosa*

Table 2. Continued.

In situ taxa	Reworked taxa
Lejeunecysta cowei	*Schematophora obscura*
Lejeunecysta acuminata	*Senegalinium* spp.
Lejeunecysta rotunda	*Spinidinium luciae*
Lejeunecysta katatonos	*Spinidinium macmurdoense*
Malvinia escutiana	*Spinidinium schellenbergii*
Nematosphaeropsis labyrinthus	*Spiniferites ramosus* cpx
Oligokolpoma galeotti	*Thalassiphora pelagica*
Operculodinium tiara	*Turbiosphaera filosa*
Operculodinium sp. A	*Turbiosphaera sagena*
Operculodinium piaseckii	*Vozzhennikovia apertura*/*S. schellenbergii* group
Operculodinium janduchenei	*Vozzhennikovia netrona*
Operculodinium cf. *eirikianum*	*?Vozzhenikovia* large
Operculodinium eirikianum	*Wetzeliella articulata*
Paleocystodinium golzowense	
Paucisphaeridium spp.	
Phthanoperidinium amoenum	
Pyxidinopsis spp. (pars)	
Pyxidinopsis sp. A	
Pyxidinopsis sp. B	
Pyxidinopsis sp. C	
Pyxidinopsis sp. D	
Pyxidinopsis vesciculata	
Pyxidinopsis tuberculata	
Pyxidinopsis reticulata	
Pyxidinopsis fairhavensis	
Reticulatosphaera actinocoronata	
Selenopemphix antarctica	
Selenopemphix nephroides	
Selenopemphix dioneacysta	
Selenopemphix sp. A	
Selenopemphix undulata	
Selenopemphix brinkhuisi	
Spiniferites sp. B	
Spiniferites sp. A	
Spiniferites sp. C	
Stoveracysta ornata	
Stoveracysta kakanuiensis	
?Svalbardella spp.	
Tectatodinium spp.	
Unipontedinium aquaeductus	
Protoperidinioid indet	
Protoperidinium sp. B	
Protoperidinium sp. A	
Protoperidinium sp. C	
Protoperidinium sp. D	

ered in situ and not reworked from older strata; Strother et al., 2017) are a constant minor (a few percent of the total palynomorph assemblage) component of the total palynomorph assemblage (Fig. 4). The terrestrial palynomorphs and the paleoclimatic and paleoecological interpretations derived from them will be presented in another study.

4.2 In situ dinocyst assemblages

Throughout the Oligocene, in situ dinocyst assemblages are dominated by protoperidinioid dinocysts, notably *Brigantedinium* spp., *Lejeunecysta* spp., *Malvinia escutiana* and *Selenopemphix* spp. (Fig. 4), all of which are cysts of heterotrophic dinoflagellates (e.g. Esper and Zonneveld, 2007). Among these protoperidinioid cysts, *S. antarctica* is fre-

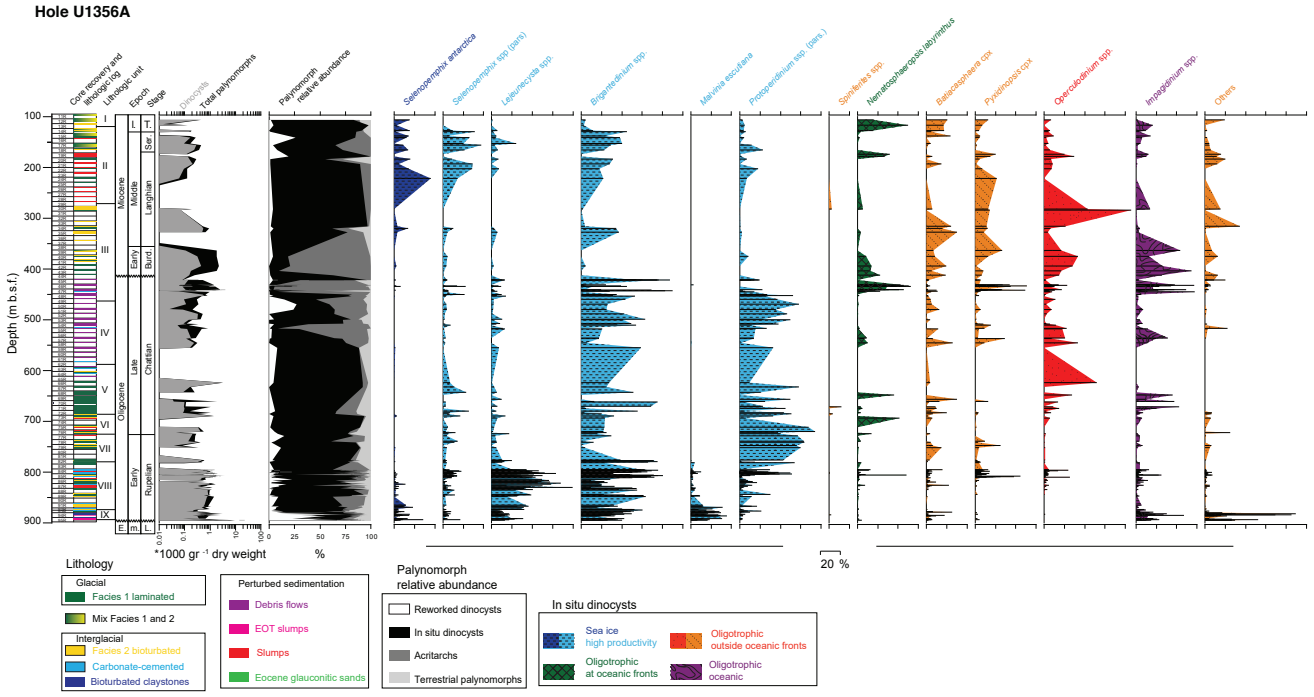

Figure 4. Core recovery, lithostratigraphic facies (after Salabarnada et al., 2018, and Sangiorgi et al., 2018), lithologic units (Escutia et al., 2011), chronostratigraphic epochs (E: Eocene) and stages (L: Lutetian; Burd.: Burdigalian; Ser.: Serravallian; T.: Tortonian), absolute palynomorph (grey) and in situ dinocyst (black) concentrations (number per gram of dry sediment, presented on a logarithmic scale), palynomorph content (reworked dinocysts, in situ dinocysts, acritarchs, terrestrial palynomorphs (given in percentages of total palynomorphs), and relative abundance of in situ dinocyst eco-groups (in percent of in situ dinocysts) for the Oligocene–Miocene of Hole U1356A.

quently present (up to 39 % of the in situ assemblage), but only between 33.6 and 32.1 Ma (earliest Oligocene) and after 14.2 Ma (i.e. during and after the mid-Miocene climatic transition, MMCT; Fig. 5). The remainder of the record is almost entirely devoid of *S. antarctica*. This is much in contrast to the dinocyst assemblages near Site U1356 today, which are dominated by this taxon (Prebble et al., 2013). Instead of *S. antarctica*, during the Oligocene and Miocene other protoperidinioid dinocysts such as *Brigantedinium* spp., several *Lejeunecysta* species and *Selenopemphix nephroides*, which have close affinities to high-nutrient conditions in general (e.g. Harland and Pudsey, 1999; Zonneveld et al., 2013) but are not specifically restricted to sea-ice proximity or the Southern Ocean, dominate. Today, these three genera dominate dinocyst assemblages in high-nutrient settings at or outside of the AAPF (Prebble et al., 2013). A varying abundance of protoperidinioid dinocysts could not be placed with confidence into established protoperidinioid dinocyst genera. These are grouped under "protoperidinium spp. (pars.)" (Fig. 4; Bijl et al., 2018a) and are here assumed to exhibit the same heterotrophic lifestyle as the other protoperidinioid dinocyst genera.

Next to protoperidinioid dinocysts, gonyaulacoid dinocysts also occur in relatively high abundances throughout the record from Site U1356. They comprise both known and previously unknown (Bijl et al., 2018a) species of *Batiacashaera*, *Pyxidinopsis*, *Corrudinium*, *Cerebrocysta*, *Nematosphaeropsis*, *Impagidinium*, *Operculodinium* and *Spiniferites* (Figs. 4, 5). The "others" group represents exclusively gonyaulacoid species such as *Invertocysta tabulata* and *Gelatia inflata*. Except for the extinct genera *Batiacasphaera* and *Cerebrocysta* and some genera in the "others" group, all the other genera are still extant and represent phototrophic dinoflagellates (Zonneveld et al., 2013). Their abundance is at the expense of the assumed heterotrophic protoperidinioid dinocysts. A marked increase in abundance of gonyaulacoid cysts is associated with the Mid-Miocene Climatic Optimum (MMCO, between ∼17 and 15 Ma; Figs. 4, 5; Sangiorgi et al., 2018). Of the gonyaulacoid taxa, *Nematosphaeropsis labyrinthus* is associated with frontal systems of the present-day Southern Ocean (Prebble et al., 2013) and of the North Atlantic Ocean (Boessenkool et al., 2001; Zonneveld et al., 2013).

4.3 Comparison between palynological data and lithological facies

The Oligocene–Miocene sediments from Site U1356 comprise distinctive alternations of lithologic facies throughout the section (Salabarnada et al., 2018; their Fig. S2). Lami-

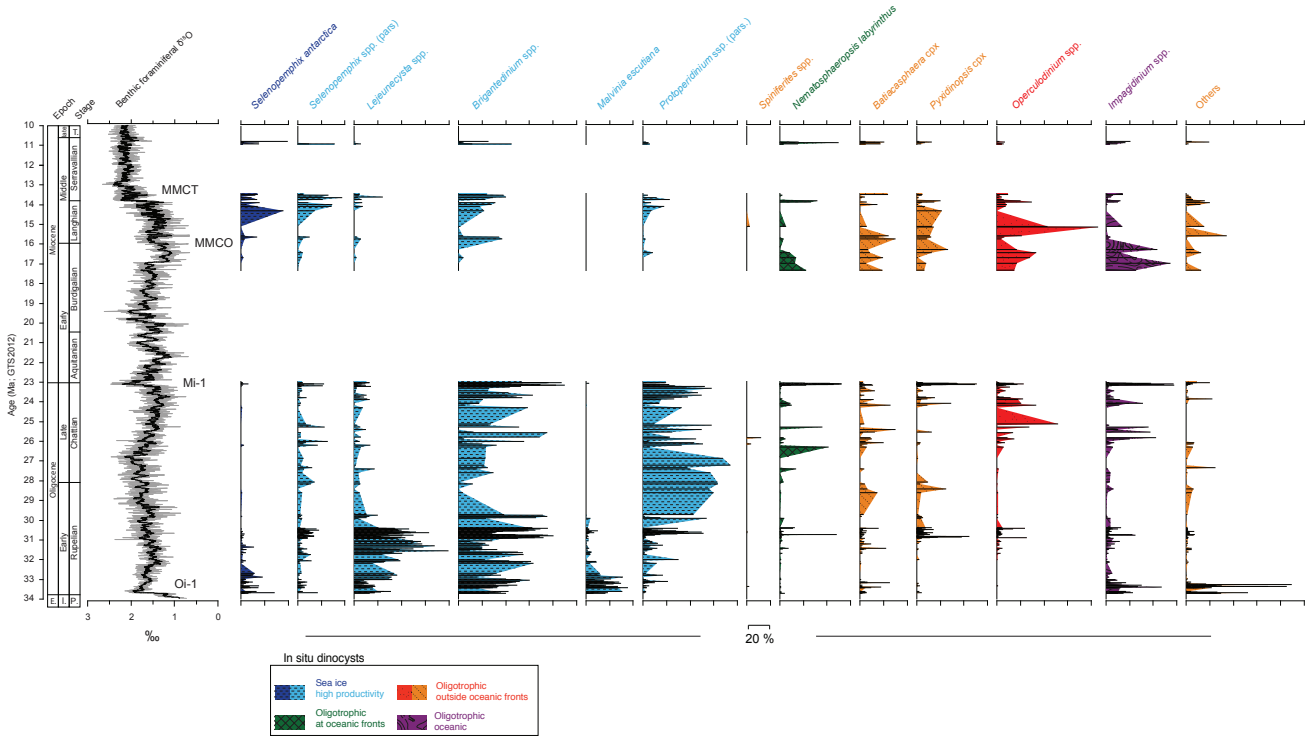

Figure 5. Megasplice of benthic foraminiferal oxygen isotope data (De Vleeschouwer et al., 2017) from Site 1146 (Holbourn et al., 2013), Site 1338, (Holbourn et al., 2014), Site 1337 (Holbourn et al., 2015), Site 1090 (Billups et al., 2004), Site 926 (Pälike et al., 2006a) and Site 1218 (Pälike et al., 2006b), with a 15-point running mean. In situ dinocyst assemblage data from Site U1356. The age–depth model specified in Fig. 2 and Table 1 was used. E.: Eocene; l.: late; P.: Priabonian; T.: Tortonian.

nated (Fg) and bioturbated sediments, which in some intervals are carbonate-rich (Fi), alternate on orbital timescales and this pattern is in some intervals disrupted by slumps and/or debris flows. Here we evaluate and compare the palynological content of each of these facies in terms of both absolute and relative abundance of the main palynomorph groups: reworked dinocysts, in situ dinocysts, acritarchs and terrestrial palynomorphs, and relative abundance of in situ dinocyst eco-groups.

4.3.1 Palynomorph groups and lithology

There are distinct differences in the relative and absolute abundances of the palynomorph groups among the different lithologies (Fig. 6). The highest relative and absolute abundances of reworked dinocysts occur in the slump and Fi facies (Fig. 6), particularly those of early Oligocene age (Eocene–Oligocene transition (EOT) slumps and bioturbated siltstones in Supplement datasets), in line with observations of Houben et al. (2013). Reworking is a minor component of the palynomorph assemblage in the other lithologies for most samples, with a higher absolute abundance in Fi deposits than in glacial deposits. This suggests that submarine erosion of Eocene continental shelf material was particularly prominent during interglacial times, when arguably sea level along the Wilkes Land margin was lower (Stocchi et al., 2013). The relative and absolute abundance of in situ dinocysts is highest in the interglacial and glacial deposits and the slumps (Fig. 6). Acritarchs reach the highest relative and absolute abundances in Fi facies and in the debris flows (Fig. 6). Terrestrial palynomorphs are most abundant in the lower Oligocene slumps and Fi sediments (Supplement tables) but have low relative abundance in all lithologies (Fig. 6).

4.3.2 In situ dinocyst eco-groups and their abundance per facies

The in situ dinocyst eco-groups are also compared with the lithological facies (Fig. 7). The Fg glacial facies contains generally more peridinioid (heterotrophic) dinocysts, while the Fi interglacial facies contains more gonyaulacoid (oligotrophic) dinocysts, but more information is to be seen when focusing on the individual eco-groups. The abundance of *Selenopemphix antarctica* is low throughout the record (0–5 %), with the exception of the interval post-dating the MMCO and the lowermost Oligocene, when the taxon occasionally reaches more than 20 % (Figs. 4, 5). *S. antarctica* reaches the highest abundances in the slump facies and Fg and is less abundant in the other lithologies (Fig. 7). *Selenopemphix* spp. reaches the highest relative abundances

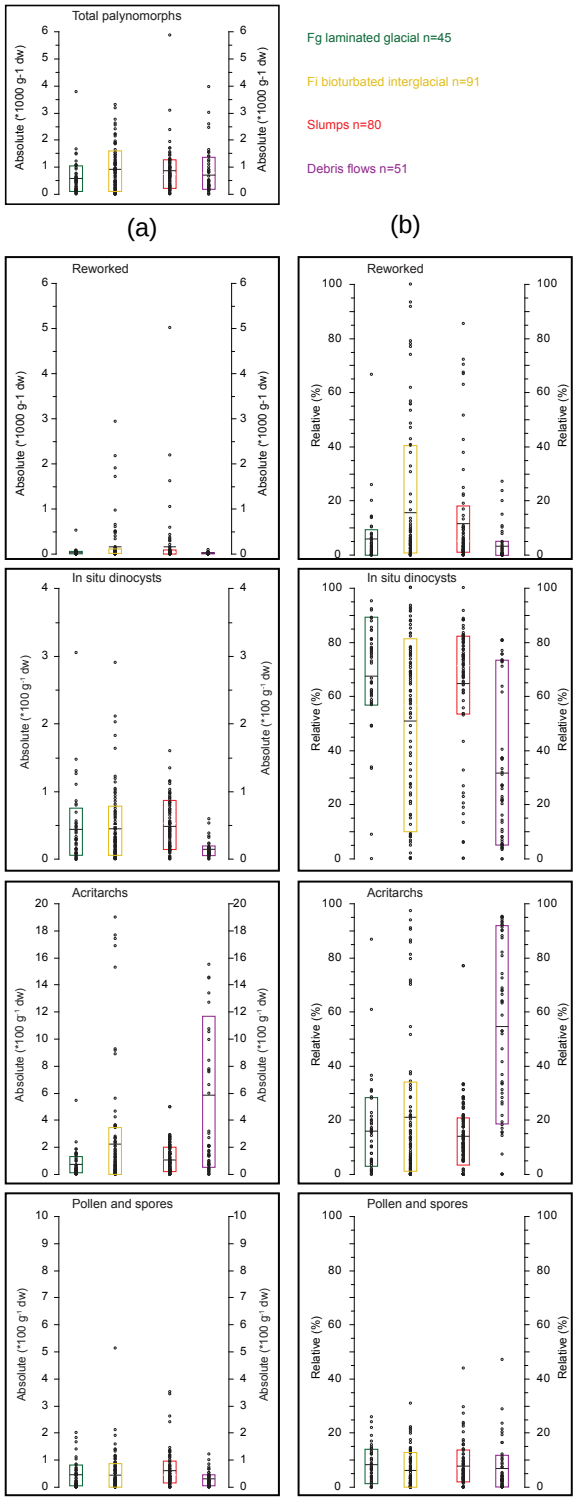

Figure 6. Comparison of absolute (**a**, in number per gram of dry weight) and relative (**b**; in percent of total palynomorphs) abundances of palynomorph groups per lithology for Hole U1356A. Average (black lines) and 17–83 % percentile (coloured bar) of absolute and relative abundances of total palynomorphs, reworked dinocysts, in situ dinocysts, acritarchs and terrestrial palynomorphs grouped for the different facies (Salabarnada et al., 2018).

in the Fg facies. *Lejeunecysta* spp. and *Protoperidinium* spp. pars. show no noticeable variance in relative abundance in any of the lithologies. *Brigantedinium* spp. is clearly more abundant in the Fg facies than in the Fi facies. *Malvinia escutiana* abundances seem to be higher in Fi than in Fg (Fig. 7), although this species has a stratigraphic occurrence that is limited to the early Oligocene (Bijl et al., 2018a). *Nematosphaeropsis labyrinthus*, *Pyxidinopsis* cpx, *Operculodinium* spp. and *Impagidinium* spp. reach higher relative abundances in the Fi than in Fg facies, whereas the abundance of *Batiacasphaera* spp. seems invariant to facies.

5 Discussion

5.1 Paleoceanographic interpretation of the dinocyst assemblages

The composition of the dinoflagellate cyst assemblages in the Wilkes Land record reflect changes in surface-ocean nutrients, sea-surface temperature conditions and paleoceanographic features. We will discuss these implications in the following.

5.1.1 Surface-ocean nutrient conditions

The general dominance of heterotrophic dinocysts in the Oligocene–Miocene assemblages indicates overall high nutrient levels in the surface waters. Given the offshore geographic setting, we therefore infer that surface waters at Site U1356 experienced upwelling associated with the AAPF during most of the Oligocene and Miocene. We can exclude the possibility that nutrients were brought to the site via river run-off given the anticipated small catchment area that experienced liquid precipitation in the Wilkes Land hinterland, the low amounts of terrestrially derived (amorphous) organic matter in the palynological residues and relatively low branched over isoprenoid tetraether (BIT) index values (Hartman et al., 2017) that indicate predominantly marine organic matter. The exception may be the MMCO (Sangiorgi et al., 2018) when considerable soil-derived organic matter reached the site.

The occasionally abundant gonyaulacoid cyst taxa encountered in our record suggest that at times surface waters that were much less nutrient-rich supported the growth of oligotrophic dinoflagellates. Notably, these taxa are typical for outer-shelf to oceanic or outer neritic settings (e.g. Sluijs et al., 2005; Zonneveld et al., 2013; Prebble et al., 2013), which makes it unlikely that they were reworked from the continental shelf. Indeed, they show low relative abundances in the perturbed deposits (Fig. 7). Although the members of these genera have relatively long stratigraphic ranges extending back into the Eocene, most of the species encountered at Site U1356 are not present in Eocene continental shelf sediments in the region (e.g. Wrenn and Hart, 1988; Levy and Harwood, 2000; Brinkhuis et al., 2003a, b; Bijl et al.,

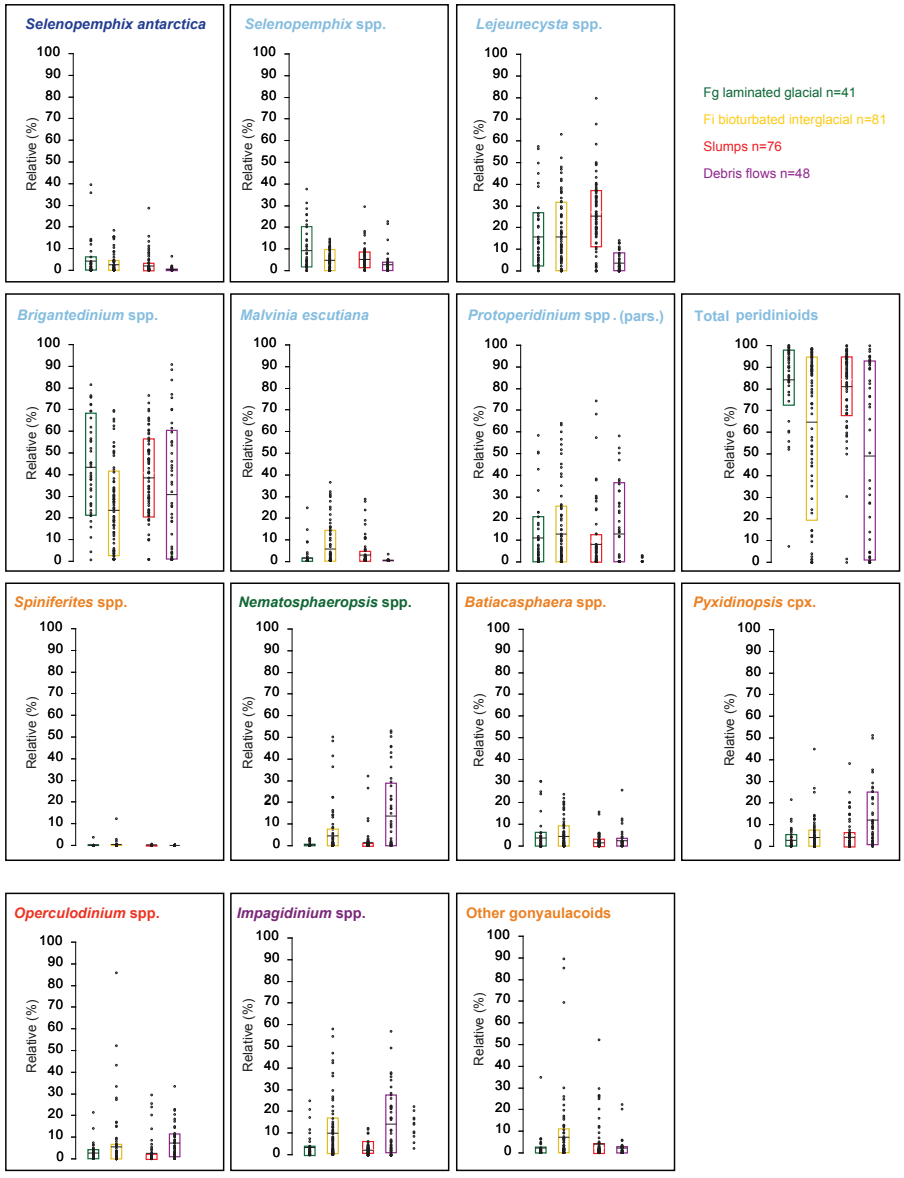

Figure 7. Relative abundance of in situ eco-groups within various lithologies at Hole U1356A. Average (black line) and 17–83 % percentile (coloured bar) of relative abundances of grouped taxa from samples from the different facies (Salabarnada et al., 2018).

2010, 2011, 2013a, b). This makes it unlikely that they are reworked from Eocene strata. In addition, statistical analysis also yields that these species are part of the in situ assemblage (Bijl et al., 2018a). These different lines of evidence lead us to interpret them as part of the in situ pelagic assemblage in our study, which allows us to interpret their paleoceanographic implications based on their modern affinities. The absence of these taxa in modern surface waters south of the AAPF is probably caused by a combination of different factors: it can be connected to low sea-surface temperatures and an isolation by strong eastward currents but also to the abundance and seasonally concentrated availability of nutrients, all of which make the proximal surface waters off Antarctica a highly specialistic niche unfavourable for these species. Apparently, surface water conditions during the Oligocene and Miocene were such that these oligotrophic species could at times proliferate so close to the Antarctic margin.

5.1.2 Sea-surface temperature

The best modern analogues for the dinocyst assemblages in our record are to be sought off the southern margins of New Zealand and Tasmania (as inferred from Prebble et al., 2013; Fig. 2). Today, these regions feature a mix between protoperidinioid dinocysts along with gonyaulacoid dinocyst genera

such as *Nematosphaeropsis*, *Operculodinium* and *Impagidinium*. These assemblages prevail in surface waters with mean annual temperatures of 8–17 °C (Prebble et al., 2013) and therefore suggest relatively warm surface water temperatures close to the Wilkes Land margin. In support of this, a Bayesian approach on the TEX_{86} index values at Site U1356 (presented in Sangiorgi et al., 2018; Hartman et al., 2017) also suggests the Southern Ocean mid-latitudes as a modern-analogue region and reconstructs a paleotemperature range of 8–20 °C for the Oligocene–Miocene at Site U1356, with values in excess of 24 °C for the late Oligocene (Hartman et al., 2017). Further, supporting evidence for temperate Oligocene–Miocene surface waters comes from the abundance of nannofossils encountered in the sediments (Escutia et al., 2011; Salabarnada et al., 2018). Today, carbonate-producing plankton is rare in high-latitude surface waters south of the AAPF (Eynaud et al., 1999). Moreover, the remains of the few pelagic carbonate-producing organisms living at high latitudes rarely reach the ocean floor because of strong upwelling of relatively CO_2-rich, corrosive waters (e.g. Olbers et al., 2004). Hence, the presence of carbonate-rich intervals during the Oligocene–Miocene at Site U1356 along with the encountered oligotrophic, temperate dinocysts suggests fundamentally warmer surface water conditions than today.

5.1.3 Surface paleoceanography

The strong similarity of Oligocene–Miocene dinocyst assemblages at Site U1356 with those today occurring much further north (i.e. around Tasmania and southern New Zealand (Prebble et al., 2013) suggests a fundamentally different modus operandi of Southern Ocean surface oceanography. The strict latitudinal separation of dinocyst assemblages in the Southern Ocean today (Prebble et al., 2013) is likely due to different surface water masses present across the oceanic fronts where strong wind-driven divergence around 60° S (known as the Antarctic Divergence; e.g. Olbers et al., 2004), strong sea-ice season and/or the vigorous ACC are in place. The strength and position of the AAPF during the Oligocene–Miocene is not well understood. General circulation model (GCM) experiments under Miocene boundary conditions suggest that west and east wind drifts prevailed south and north of 60° S, respectively (Herold et al., 2011). This wind orientation determined the average position of the Antarctic Divergence at 60° S during the Oligocene and Miocene, similar to today. This suggests that Site U1356 was likely directly overlain by the AAPF. However, the significantly warmer, more oligotrophic dinocyst assemblages off Wilkes Land throughout the Oligocene–Miocene argue against proximity to the AAPF. The position of the AAPF relative to that of Site U1356 strongly determines the likelihood of southward transport of low-latitude waters towards the site. A southward position of the AAPF relative to Site U1356 would greatly enhance the possibility for a southward migration of temperate surface water masses towards the site. A northward position of the AAPF relative to the site would make such a latitudinal migration much more difficult. The presence of carbonate in these deep marine sediments also suggests that upwelling of corrosive waters through the (proto-)Antarctic Divergence was either much reduced or located elsewhere. Therefore, we deduce that the occurrence of the oligotrophic, temperate dinocysts is evidence for a southward position of the AAPF relative to the position of Site U1356. This would allow a higher connectivity between the site and the lower latitudes and promote preservation of carbonate on the sea floor. Also, such an oceanographic setting would be in line with reduced sea ice along the Wilkes Land margin.

The separate averaging of dinocyst assemblages for glacial and interglacial facies from Site U1356 (Fig. 7) allows us to reconstruct glacial–interglacial changes in surface water conditions throughout the Oligocene. First of all, our observations suggest that Oligocene glacial–interglacial cycles were connected to substantial paleoceanographic dynamics off Wilkes Land. In agreement with the 2–3 °C SST variability as documented for this site during glacial–interglacial cycles (Hartman et al., 2017), dinocyst assemblages contain more oligotrophic, temperate dinocysts during interglacial times compared to glacial times when more eutrophic, colder dinocysts proliferated (Fig. 7). This could be the result of a slight latitudinal movement of oceanic frontal systems (notably the AAPF) as it has been reconstructed for the Southern Ocean fronts during the most recent glacial-to-interglacial transition (e.g. Bard and Rickaby, 2009; Kohfeld et al., 2013; Xiao et al., 2016). In such a scenario, the AAPF would reach a southern position during interglacials, allowing for temperate oligotrophic surface waters to reach the site, while it would migrate northward over Site U1356 during glacials, thereby causing cold, high-nutrient surface water conditions and obstructing low-latitude influence.

5.2 Implications for Oligocene–Miocene ocean circulation

At Site U1356, dinocyst assemblages bear similarities to present-day proximal-Antarctic assemblages (Prebble et al., 2013) only in the lowermost Oligocene and in strata deposited after the MMCO (after 14.2 Ma); in particular, they are characterized by high abundances (up to 39 %) of *Selenopemphix antarctica*. Even in those intervals, however, the relative abundances of *S. antarctica* do not reach present-day values at the same site (Prebble et al., 2013). The absence of a strong shift towards modern-day-like assemblages in our record can be interpreted to reflect a weaker-than-present ACC. This interpretation is in line with numerical models (Herold et al., 2012; Hill et al., 2013). The ACC itself represents an important barrier for latitudinal surface water transport towards the Antarctic margin, in addition to the Antarctic Divergence (Olbers et al., 2004). Our data suggest

an increase in the influence of oligotrophic dinocysts at the Antarctic margin during the late Oligocene and during the MMCO, which argues against the installation of a vigorous ACC at 30 Ma as recently inferred by Scher et al. (2015): No particular change in sea-surface conditions emerges from our dinoflagellate cyst data around 30 Ma, and there is no major change in the benthic δ^{18}O data either (Fig. 5). Instead, if the Tasmanian Gateway had opened to an extent that allowed ACC development (Scher et al., 2015), the ACC must have been much weaker throughout the Oligocene and Miocene than at present, which has also emerged from modelling experiments (Hill et al., 2013). The strongly different dinocyst assemblages compared to present-day dinocyst assemblages near Site U1356 throughout our record imply that a strong coherent ACC was not installed until after the MMCT (11 Ma). This is consistent with inferences from the lithology at the same site (Salabarnada et al., 2018), suggesting a proto-ACC much weaker than at present and, likewise, weaker Southern Ocean frontal systems. An alternative explanation is that the ACC increased in strength during the Oligocene–Miocene, but that this strengthening had no influence on the dinocyst assemblages at Site U1356. However, the vigorous nature of the ACC influencing surface as well as bottom waters and governing eddy water circulation in the Southern Ocean (Olbers et al., 2004) in combination with the high sensitivity of dinoflagellates to changes in surface water conditions (e.g. Zonneveld et al., 2013; Prebble et al., 2013) makes such a scenario very unlikely. Nevertheless, to firmly clarify whether the ACC reached its present-day strength only after the MMCT (as suggested by our data), ocean-circulation modelling of time slices younger than the Oligocene (Hill et al., 2013) will be required.

Our results also seem difficult to reconcile with indications of bottom-water formation at the Wilkes Land margin, as seen from neodymium isotope analyses on the same sediments (Huck et al., 2017). It could be that bottom-water formation took place only when surface waters cooled down in wintertime, and the organic proxies are more representative of spring–summer conditions. Salabarnada et al. (2018) interpret bottom-current activity in the Oligocene at Site U1356 and suggest it may be spilling over from the Ross Sea, like today. Our dinocyst results and the SST reconstructions by Hartman et al. (2017) suggest that surface waters at the Wilkes Land margin were too warm to allow local bottom-water formation; therefore our data also support the suggestion that bottom water along the Wilkes Land margin was sourced from the Ross Sea.

5.3 Implications for ice-sheet and sea-ice variability

The relative abundances of the sea-ice-related *Selenopemphix antarctica* are consistently lower in our record than in present-day dinocyst assemblages near Site U1356 (Prebble et al., 2013; Fig. 3). This suggests that sea-ice conditions were never similar to today during the studied time interval. More specifically, our dinocysts suggest the occurrence of sea ice near the site only during two time intervals: the first 1.5 million years following the Oi-1 glaciation (33.6–32.1 Ma; Fig. 5), and during and after the MMCT (after 14.2 Ma; Fig. 5). Numerical ice-sheet and sea-ice modelling (DeConto et al., 2007) has suggested sea ice to develop only if the continental ice sheets reach the coastline. Our lack of sea-ice indicators during most of the Oligocene and Miocene could thus point towards a much-reduced Antarctic continental ice sheet during that time. The finding of a weaker sea-ice season throughout most of the Oligocene–Miocene at Site U1356 is important because it suggests a decrease in the potential formation of Antarctic bottom waters at this site.

The relative abundance of oligotrophic dinocyst taxa broadly follows long-term Oligocene–Miocene benthic δ^{18}O trends (see Fig. 5): during times of low δ^{18}O values in deep-sea benthic foraminifera (and thus high deep-sea temperatures and/or less ice volume, e.g. at 32, 24 and 15 Ma; Fig. 5), the abundance of oligotrophic temperate dinocysts was high (Fig. 5). At times of higher δ^{18}O values, lower deep-sea temperatures and higher ice volume (e.g. at 33.5, 27, 23, and 13 Ma; Fig. 5), temperate dinocysts were reduced in abundance and high-nutrient, sea-ice indicators (re)appeared. Altogether, on long timescales this pattern suggests that there was a stronger influence of warm surface waters at the Wilkes Land margin at times when ice sheets were smaller and climate was warmer and less influence of warm surface waters during times of larger ice sheets. Hence a connection existed between ice-sheet expansion–retreat and paleoceanography.

Oxygen-isotope mass-balance calculations suggest that a modern-day-sized Antarctic ice sheet formed at the Eocene–Oligocene boundary (DeConto et al., 2008). Benthic δ^{18}O records suggest that ice sheets must have fluctuated considerably in size during the subsequent Oligocene and Miocene (Liebrand et al., 2017), although this inference lacks an independent assessment of the deep-sea temperature effect in these δ^{18}O values. The same conclusion was reached based on detailed microfossil, geochemical and facies analyses on sediments from the Gippsland Basin, southeast Australia (Gallagher et al., 2013). This study suggests that ice volume during the early Oligocene varied by as much as 140–40 % of its present-day size, of which the maximum ice volume estimates far exceed those implied by our data. However, there is consistency in the observation of considerable glacial–interglacial and long-term dynamics in the ice–ocean system. This is in contrast to the heavy δ^{18}O values for Oligocene benthic foraminifera from Maud Rise (ODP Site 690), which suggest Antarctic ice sheets were near present-day size throughout the Oligocene (Hauptvogel et al., 2017). It remains to be seen whether the variability in paleoceanography as indicated by our data can be extrapolated to larger parts of the Antarctic margin, including regions of deep-water formation. Given the high temperatures and only weak sea-ice influence, the Wilkes Land margin was likely not the primary sector of deep-water formation

(see, e.g. Herold et al., 2012), although there is ample evidence for bottom-current activity at the site (Salabarnada et al., 2018; Huck et al., 2017). Instead, it appears that bottom-water formation during the Oligocene took place along the Wilkes Land coast (Huck et al., 2017). If the oceanographic and climate variability that we reconstruct offshore Wilkes Land also characterises regions of deep-water formation, some (if not all) of the variability on both long and orbital timescales as documented in benthic δ^{18}O records would be due to changes in deep-sea temperature rather than Antarctic ice volume (see also Hartman et al., 2017). Meanwhile, we find little support in our study for the large (and, by implication, marine-terminating) continental ice sheets in this sector of East Antarctica during the Oligocene as implied by Hauptvogel et al. (2017) given the absence of dominance of sea-ice dinocysts and the presence of in situ terrestrial palynomorphs (Strother et al., 2017). As an alternative explanation for the difference in δ^{18}O values between Maud Rise (Site 690) and the equatorial Pacific (Site 1218) during the Oligocene (Hauptvogel et al., 2017), we suggest that these two sedimentary archives have recorded the characteristics of two different deep-water masses, with those at Maud Rise (Site 690) being much colder and more saline than those in the equatorial Pacific (Site 1218).

6 Conclusions

The dinocyst assemblages in the Oligocene–Miocene (33.6–11 Ma) of Site U1356 were interpreted in terms of surface water paleoceanography via comparison with present-day dinocyst distribution patterns. Based on our results, we suggest that the Oligocene–Miocene surface paleoceanography of the Southern Ocean was fundamentally different from that of today. A sea-ice signal (weaker still than at present) emerges for the Wilkes Land margin only for the first 1.5 million years of the Oligocene (33.6–32.1 Ma) and during and after the MMCT (after 14.2 Ma). During the remainder of the Oligocene–Miocene, surface waters off Wilkes Land were warm and relatively oligotrophic; notably, they lack indications of a prominent sea-ice season. Upwelling at the Antarctic Divergence was profoundly weaker during Oligocene and Miocene times than at present, or significantly displaced southward from its present-day position. Furthermore, the continental ice sheets were much reduced at the Wilkes Land subglacial basin for most of the Oligocene–Miocene compared to today. The influence of warm oligotrophic surface waters appears strongly coupled to deep-sea δ^{18}O values, suggesting enhanced low-latitude influence of surface waters during times of light δ^{18}O in the deep sea and vice versa. The absence of (a trend towards a stronger) paleoceanographic isolation of the Wilkes Land margin throughout the Oligocene to mid-Miocene suggests that the ACC may not have attained its full, present-day strength until at least after the mid-Miocene climatic transition. Moreover, we note considerable glacial–interglacial amplitude variability in this oceanographic setting. Stronger influence of oligotrophic, low-latitude-derived surface waters prevailed over Site U1356 during interglacial times and more eutrophic, colder waters during glacial times. This pattern may suggest considerable latitudinal migration of the AAPF over the course of Oligocene and Miocene glacial–interglacial cycles.

Data availability. The datasets to this article are available at PANGAEA (Bijl et al., 2018b) and in the Supplement.

Supplement. The supplement related to this article is available online at: https://doi.org/10.5194/cp-14-1015-2018-supplement.

Author contributions. PKB, FS, CE and JP designed the research. AJPH, FS and PKB carried out dinocyst analyses for the earliest Oligocene, the Miocene and the Oligocene–Miocene boundary interval, respectively. AS and CE provided the lithological data. PKB integrated, cross-validated, and compiled the data and wrote the paper with input from all co-authors.

Competing interests. The authors declare that they have no conflict of interest.

Acknowledgements. This research used data and samples from the Integrated Ocean Drilling Program (IODP). IODP was sponsored by the US National Science Foundation and participating countries under management of Joined Oceanographic Institutions Inc. Peter K. Bijl and Francesca Sangiorgi thank NWO-NNPP grant no. 866.10.110 and NWO-ALW VENI grant no. 863.13.002 for funding and Natasja Welters for technical support. Jörg Pross acknowledges support through the IODP priority program of the German Research Foundation (DFG). Carlota Escutia and Ariadna Salabarnada thank the Spanish Ministerio de Economía y Competitividad for grant CTM2014-60451-C2-1-P. We thank Kasia Śliwińska, Stephen Gallagher and the anonymous reviewer for their constructive comments that considerably improved our paper.

Edited by: David Thornalley
Reviewed by: Stephen Gallagher, Kasia K. Śliwińska, and one anonymous referee

References

Badger, M. P. S., Lear, C. H., Pancost, R. D., Foster, G. L., Bailey, T. R., Leng, M. J., and Abels, H. A.: CO_2 drawdown following the middle Miocene expansion of the Antarctic Ice Sheet, Paleoceanography, 28, 42–53, 2013.

Bard, E. and Rickaby, R. E. M.: Migration of the subtropical front as a modulator of glacial climate, Nature, 460, 380–383, 2009.

Barker, P., Camerlenghi, A., Acton, G., Brachfeld, S., Cowan, E., Daniels, J., Domack, E., Escutia, C., Evans, A., Eyles, N., Guyodo, Y., Iorio, M., Iwai, M., Kyte, F., Lauer, C., Maldonado, A., Moerz, T., Osterman, L., Pudsey, C., Schuffert, J., Sjunneskog, C., Vigar, K., Weinheimer, A., Williams, T., Winter, D., and Wolf-Welling, T.: Antarctic glacial history and sea-level change – Leg 178 samples Antarctic Peninsula margin sediments, JOIDES Journal, 24, 7–10, 1998.

Barker, P. F. and Thomas, E.: Origin, signature and paleoclimatic influence of the Antarctic Circumpolar Current, Earth-Sci. Rev., 66, 143–162, 2004.

Barker, P. F., Barrett, P. J., Cooper, A. K., and Huybrechts, P.: Antarctic glacial history from numerical models and continental margin sediments, Palaeogeogr. Palaeocl., 150, 247–267, 1999.

Barrett, P. J.: Antarctic Cenozoic history from the CIROS-1 drillhole, McMurdo Sound, Science Information Publishing Centre DSIR Bulletin, 245, Wellington, 1989.

Beddow, H. M., Liebrand, D., Sluijs, A., Wade, B. S., and Lourens, L. J.: Global change across the Oligocene-Miocene transition: High-resolution stable isotope records from IODP Site U1334 (equatorial Pacific Ocean), Paleoceanography, 31, 81–97, 2016.

Bijl, P. K., Houben, A. J. P., Schouten, S., Bohaty, S. M., Sluijs, A., Reichart, G. J., Sinninghe Damsté, J. S., and Brinkhuis, H.: Transient Middle Eocene Atmospheric Carbon Dioxide and Temperature Variations, Science, 330, 819–821, 2010.

Bijl, P. K., Pross, J., Warnaar, J., Stickley, C. E., Huber, M., Guerstein, R., Houben, A. J. P., Sluijs, A., Visscher, H., and Brinkhuis, H.: Environmental forcings of Paleogene Southern Ocean dinoflagellate biogeography, Paleoceanography, 26, PA1202, https://doi.org/10.1029/2009PA001905, 2011.

Bijl, P. K., Bendle, A. P. J., Bohaty, S. M., Pross, J., Schouten, S., Tauxe, L., Stickley, C. E., McKay, R. M., Röhl, U., Olney, M., Sluijs, A., Escutia, C., Brinkhuis, H., and Expedition 318 scientists: Eocene cooling linked to early flow across the Tasmanian Gateway, P. Natl. Acad. Sci. USA, 110, 9645–9650, 2013a.

Bijl, P. K., Sluijs, A., and Brinkhuis, H.: A magneto-chemostratigraphically calibrated dinoflagellate cyst zonation of the early Paleogene South Pacific Ocean, Earth-Sci. Rev., 124, 1–31, 2013b.

Bijl, P. K., Houben, A. J. P., Bruls, A., Pross, J., and Sangiorgi, F.: Stratigraphic calibration of Oligocene–Miocene organic-walled dinoflagellate cysts from offshore Wilkes Land, East Antarctica, and a zonation proposal, J. Micropalaeontol., 37, 105–138, https://doi.org/10.5194/jm-37-105-2018, 2018a.

Bijl, P. K., Houben, A. J. P., Hartmann, J. D., Pross, J., Salabarnada, A., Escutia, C., and Sangiorgi, F.: Palynological counts from the Oligocene-Miocene of IODP Site 318-U1356, Wilkes Land Margin, Antarctica, PANGAEA, https://doi.org/10.1594/PANGAEA.890160, 2018b.

Billups, K., Pälike, H., Channell, J. E. T., Zachos, J. C., and Shackleton, N. J.: Astronomic calibration of the late Oligocene through early Miocene geomagnetic polarity time scale, Earth Planet. Sc. Lett., 224, 33–44, 2004.

Boessenkool, K. P., Van Gelder, M., Brinkhuis, H., and Troelstra, S. R.: Distribution of organic-walled dinoflagellate cysts in surface sediments from transects across the Polar Front offshore southeast Greenland, J. Quaternary Sci., 16, 661–666, 2001.

Brinkhuis, H., Munsterman, D. M., Sengers, S., Sluijs, A., Warnaar, J., and Williams, G. L.: Late Eocene to Quaternary dinoflagellate cysts from ODP Site 1168, off western Tasmania, in: Proceedings of the Ocean Drilling Program, Scientific Results, edited by: Exon, N. and Kennett, J. P., 189, U.S. Government Printing Office, College Station, Texas, 2003a.

Brinkhuis, H., Sengers, S., Sluijs, A., Warnaar, J., and Williams, G. L.: Latest Cretaceous to earliest Oligocene, and Quaternary dinoflagellates from ODP Site 1172, East Tasman Plateau, in: Proceedings of the Ocean Drilling Program, Scientific Results, edited by: Exon, N. and Kennett, J. P., 189, U.S. Government Printing Office, College Station, Texas, 2003b.

Close, D. I., Watts, A. B., and Stagg, H. M. J.: A marine geophysical study of the Wilkes Land rifted continental margin, Antarctica, Geophys. J. Int., 177, 430–450, 2009.

Cook, C. P., Van De Flierdt, T., Williams, T., Hemming, S. R., Iwai, M., Kobayashi, M., Jimenez-Espejo, F. J., Escutia, C., González, J. J., Khim, B., McKay, R. M., Passchier, S., Bohaty, S. M., Riesselman, C. R., Tauxe, L., Sugisaki, S., Galindo, A. L., Patterson, M. O., Sangiorgi, F., Pierce, E. L., Brinkhuis, H., Klaus, A., Fehr, A., Bendle, J. A. P., Bijl, P. K., Carr, S. A., Dunbar, R. B., Flores, J. A., Hayden, T. G., Katsuki, K., Kong, G. S., Nakai, M., Olney, M. P., Pekar, S. F., Pross, J., Röhl, U., Sakai, T., Shrivastava, P. K., Stickley, C. E., Tuo, S., Welsh, K., and Yamane, M.: Dynamic behaviour of the East Antarctic ice sheet during Pliocene warmth, Nat. Geosci., 6, 765–769, 2013.

Cooper, A. K. and O'Brien, P. E.: Leg 188 synthesis: Transitions in the glacial history of the Prydz Bay region, East Antarctica, from ODP drilling, Proceedings of the Ocean Drilling Program: Scientific Results, 188, 1–42, 2004.

Crampton, J. S., Cody, R. D., Levy, R., Harwood, D., McKay, R., and Naish, T. R.: Southern Ocean phytoplankton turnover in response to stepwise Antarctic cooling over the past 15 million years, P. Natl. Acad. Sci. USA, 113, 6868–6873, 2016.

DeConto, R. M., Pollard, D., and Harwood, D.: Sea-ice feedback and Cenozoic evolution of Antarctic climate and ice sheets, Paleoceanography, 22, PA3214, https://doi.org/10.1029/2006PA001350, 2007.

DeConto, R. M., Pollard, D., Wilson, P. A., Pälike, H., Lear, C. H., and Pagani, M.: Thresholds for Cenozoic bipolar glaciation, Nature, 455, 652–657, 2008.

De Vleeschouwer, D., Vahlenkamp, M., Crucifix, M., and Pälike, H.: Alternating Southern and Northern Hemisphere climate response to astronomical forcing during the past 35 m.y., Geology, 45, 375–378, 2017.

Egger, L. M., Bahr, A., Friedrich, O., Wilson, P. A., Norris, R. D., van Peer, T. E., Lippert, P. C., Liebrand, D., and Pross, J.: Sea-level and surface-water change in the western North Atlantic across the Oligocene–Miocene Transition: a palynological perspective from IODP Site U1406 (Newfoundland margin), Mar. Micropaleontol., 139, 57–71, 2018.

Escutia, C. and Brinkhuis, H.: From Greenhouse to Icehouse at the Wilkes Land Antarctic Margin: IODP Expedition 318 Synthesis of Results, Dev. Mar. Geol., 7, 295–328, 2014.

Escutia, C., Brinkhuis, H., Klaus, A., and Expedition 318 Scientists: Proceedings of the Integrated Ocean Drilling Program, Initial Results, 318, Integrated Ocean Drilling Program Management International, Inc., Tokyo, 2011.

Esper, O. and Zonneveld, K. A. F.: Distribution of organic-walled dinoflagellate cysts in surface sediments of the Southern Ocean

(eastern Atlantic sector) between the Subtropical Front and the Weddell Gyre, Mar. Micropaleotol., 46, 177–208, 2002.

Esper, O. and Zonneveld, K. A. F.: The potential of organic-walled dinoflagellate cysts for the reconstruction of past sea-surface conditions in the Southern Ocean, Mar. Micropaleontol., 65, 185–212, 2007.

Exon, N. F., Kennet, J. P., and Malone, M.: Leg 189 Synthesis: Cretaceous-Holocene history of the Tasmanian Gateway, in: Proceedings of the Ocean Drilling Program, Scientific Results, edited by: Exon, N. F., Kennett, J. P., and Malone, M. J., 189, Ocean Drilling Program, College Station, TX, USA, 2004.

Eynaud, F., Giraudeau, J., Pichon, J., and Pudsey, C. J.: Sea-surface distribution of coccolithophores, diatoms, silicoflagellates and dinoflagellates in the South Atlantic Ocean during the late austral summer 1995, Deep-Sea Res. Pt. I, 46, 451–482, 1999.

Foster, G. L. and Rohling, E. J.: Relationship between sea level and climate forcing by CO_2 on geological timescales, P. Natl. Acad. Sci. USA, 110, 1209–1214, 2013.

Foster, G. L., Lear, C. H., and Rae, J. W. B.: The evolution of pCO_2, ice volume and climate during the middle Miocene, Earth Planet. Sc. Lett., 341–344, 243–254, 2012.

Fretwell, P., Pritchard, H. D., Vaughan, D. G., Bamber, J. L., Barrand, N. E., Bell, R., Bianchi, C., Bingham, R. G., Blankenship, D. D., Casassa, G., Catania, G., Callens, D., Conway, H., Cook, A. J., Corr, H. F. J., Damaske, D., Damm, V., Ferraccioli, F., Forsberg, R., Fujita, S., Gim, Y., Gogineni, P., Griggs, J. A., Hindmarsh, R. C. A., Holmlund, P., Holt, J. W., Jacobel, R. W., Jenkins, A., Jokat, W., Jordan, T., King, E. C., Kohler, J., Krabill, W., Riger-Kusk, M., Langley, K. A., Leitchenkov, G., Leuschen, C., Luyendyk, B. P., Matsuoka, K., Mouginot, J., Nitsche, F. O., Nogi, Y., Nost, O. A., Popov, S. V., Rignot, E., Rippin, D. M., Rivera, A., Roberts, J., Ross, N., Siegert, M. J., Smith, A. M., Steinhage, D., Studinger, M., Sun, B., Tinto, B. K., Welch, B. C., Wilson, D., Young, D. A., Xiangbin, C., and Zirizzotti, A.: Bedmap2: improved ice bed, surface and thickness datasets for Antarctica, The Cryosphere, 7, 375–393, https://doi.org/10.5194/tc-7-375-2013, 2013.

Gallagher, S. J., Villa, G., Drysdale, R. N., Wade, B. S., Scher, H., Li, Q., Wallace, M. W., and Holdgate, G. R.: A near-field sea level record of east Antarctic ice sheet instability from 32 to 27 Myr, Paleoceanography, 28, 1–13, 2013.

Gradstein, F. M., Ogg, J. G., Schmitz, M. D., and Ogg, G. M.: The Geologic Time Scale 2012, Elsevier, Amsterdam, the Netherlands, 1–2, 1–1144, 2012.

Greenop, R., Foster, G. L., Wilson, P. A., and Lear, C. H.: Middle Miocene climate instability associated with high-amplitude CO_2 variability, Paleoceanography, 29, 845–853, 2014.

Harland, R. and Pudsey, C. J.: Dinoflagellate cysts from sediment traps deployed in the Bellingshausen, Weddell and Scotia seas, Antarctica, Mar. Micropaleontol., 37, 77–99, 1999.

Hartman, J. D., Sangiorgi, F., Salabarnada, A., Peterse, F., Houben, A. J. P., Schouten, S., Escutia, C., and Bijl, P. K.: Oligocene TEX_{86}-derived seawater temperatures from offshore Wilkes Land (East Antarctica), Clim. Past Discuss., https://doi.org/10.5194/cp-2017-153, in review, 2017.

Harwood, D., Levy, R., Cowie, J., Florindo, F., Naish, T., Powell, R., and Pyne, A.: Deep Drilling with the ANDRILL Program in Antarctica, Sci. Dril., 3, 43–45, https://doi.org/10.2204/iodp.sd.3.09.2006, 2006.

Hauptvogel, D. W., Pekar, S. F., and Pincay, V.: Evidence for a heavily glaciated Antarctica during the late Oligocene "warming" (27.8–24.5): stable isotope records from ODP Site 690, Paleoceanography, 32, 384–396, 2017.

Herold, N., Huber, M., and Müller, R. D.: Modeling the Miocene Climatic Optimum. Part I: Land and atmosphere, J. Climate, 24, 6353–6373, 2011.

Herold, N., Huber, M., Müller, R. D., and Seton, M.: Modeling the Miocene Climatic Optimum: Ocean circulation, Paleoceanography, 27, PA1209, https://doi.org/10.1029/2010PA002041, 2012.

Hill, D. J., Haywood, A. M., Valdes, P. J., Francis, J. E., Lunt, D. J., Wade, B. S., and Bowman, V. C.: Paleogeographic controls on the onset of the Antarctic circumpolar current, Geophys. Res. Lett., 40, 5199–5204, 2013.

Holbourn, A., Kuhnt, W., Schulz, M., Flores, J., and Andersen, N.: Orbitally-paced climate evolution during the middle Miocene "Monterey" carbon-isotope excursion, Earth Planet. Sc. Lett., 261, 534–550, 2007.

Holbourn, A., Kuhnt, W., Clemens, S., Prell, W., and Andersen, N.: Middle to late Miocene stepwise climate cooling: Evidence from a high-resolution deep water isotope curve spanning 8 million years, Paleoceanography, 28, 688–699, 2013.

Holbourn, A., Kuhnt, W., Lyle, M., Schneider, L., Romero, O., and Andersen, N.: Middle Miocene climate cooling linked to intensification of eastern equatorial Pacific upwelling, Geology, 42, 19–22, 2014.

Holbourn, A., Kuhnt, W., Kochhann, K. G. D., Andersen, N., and Meier, K. J.: Global perturbation of the carbon cycle at the onset of the Miocene Climatic Optimum, Geology, 43, 123–126, 2015.

Houben, A. J. P., Bijl, P. K., Pross, J., Bohaty, S. M., Passchier, S., Stickley, C. E., Röhl, U., Sugisaki, S., Tauxe, L., Van De Flierdt, T., Olney, M., Sangiorgi, F., Sluijs, A., Escutia, C., and Brinkhuis, H.: Reorganization of Southern Ocean plankton ecosystem at the onset of Antarctic glaciation, Science, 340, 341–344, 2013.

Huck, C. E., van de Flierdt, T., Bohaty, S. M., and Hammond, S. J.: Antarctic climate, Southern Ocean circulation patterns, and deep water formation during the Eocene, Paleoceanography, 32, 674–691, 2017.

IPCC: Climate Change 2013: The Physical Science Basis, Contribution of Working Group I to the Fifth Assessment Report of the Intergovernmental Panel on Climate Change, Cambridge University Press, Cambridge, United Kingdom and New York, NY, USA, 2013.

Kohfeld, K. E., Graham, R. M., de Boer, A. M., Sime, L. C., Wolff, E. W., Le Quéré, C., and Bopp, L.: Southern Hemisphere westerly wind changes during the Last Glacial Maximum: paleo-data synthesis, Quaternary Sci. Rev., 68, 76–95, 2013.

Lear, C. H., Rosenthal, Y. Coxall, H. K., and Wilson, P. A.: Late Eocene to early Miocene ice sheet dynamics and the global carbon cycle, Paleoceanography, 19, PA4015, https://doi.org/10.1029/2004PA001039, 2004.

Levy, R. H. and Harwood, D. M.: Tertiary marine palynomorphs from the McMurdo Sound erratics, Antarctica, in: Paleobiology and Paleoenvironments of Eocene rocks, McMurdo Sound, East Antarctica, edited by: Stilwell, J. D. and Feldmann, R. M., AGU Antarctic Research Series, 183–242, 2000.

Liebrand, D., Lourens, L. J., Hodell, D. A., de Boer, B., van de Wal, R. S. W., and Pälike, H.: Antarctic ice sheet and oceanographic

response to eccentricity forcing during the early Miocene, Clim. Past, 7, 869–880, https://doi.org/10.5194/cp-7-869-2011, 2011.

Liebrand, D., de Bakker, A. T. M., Beddow, H. M., Wilson, P. A., Bohaty, S. M., Ruessink, G., Pälike, H., Batenburg, S. J., Hilgen, F. J., Hodell, D. A., Huck, C. E., Kroon, D., Raffi, I., Saes, M. J. M., van Dijk, A. E., and Lourens, L. J.: Evolution of the early Antarctic ice ages, P. Natl. Acad. Sci. USA, 110, 3867–3872, 2017.

Marret, F. and De Vernal, A.: Dinoflagellate cyst distribution in surface sediments of the southern Indian Ocean, Mar. Micropaleontol., 29, 367–392, 1997.

Olbers, D., Borowski, D., Völker, C., and Wölff, J.: The dynamical balance, transport and circulation of the Antarctic Circumpolar Current, Antarct. Sci., 16, 439–470, 2004.

Pälike, H., Frazier, J., and Zachos, J. C.: Extended orbitally forced palaeoclimatic records from the equatorial Atlantic Ceara Rise, Quaternary Sci. Rev., 25, 3138–3149, 2006a.

Pälike, H., Norris, R. D., Herrle, J. O., Wilson, P. A., Coxall, H. K., Lear, C. H., Shackleton, N. J., Tripati, A. K., and Wade, B. S.: The Heartbeat of the Oligocene Climate System, Science, 314, 1894–1898, 2006b.

Prebble, J. G., Crouch, E. M., Carter, L., Cortese, G., Bostock, H., and Neil, H.: An expanded modern dinoflagellate cyst dataset for the Southwest Pacific and Southern Hemisphere with environmental associations, Mar. Micropaleontol., 101, 33–48, 2013.

Rignot, E., Jacobs, S., Mouginot, J., and Scheuchl, B.: Ice-shelf melting around Antarctica, Science, 341, 266–270, 2013.

Robert, C., Anderson, J., Armienti, P., Atkins, C., Barrett, P., Bohaty, S., Bryce, S., Claps, M., Curran, M., Davey, F. J., De Santis, L., Ehrmann, W., Florindo, F., Fielding, C., Hambrey, M., Hannah, M., Harwood, D. M., Henrys, S., Hoelscher, F., Howe, J. A., Jarrard, R., Kettler, R., Kooyman, S., Kopsch, C., Krissek, L., Lavelle, M., Levac, E., Niessen, F., Passchier, S., Paulsen, T., Powell, R., Pyne, A., Rafat, G., Raine, I. J., Roberts, A. P., Sagnotti, L., Sandroni, S., Scholz, E., Simes, J., Smellie, J., Strong, P., Tabecki, M., Talarico, F. M., Taviani, M., Verosub, K. L., Villa, G., Webb, P. N., Wilson, G. S., Wilson, T., Wise, S. W., Wonik, T., Woolfe, K., and Wrenn, J. H.: Summary of Results from CRP-1, Cape Roberts Project, Antarctica, Terra Antarctica, 5, 125–137, 1998.

Rovere, A., Raymo, M. E., Mitrovica, J. X., Hearty, P. J., O'Leary, M. J., and Inglis, J. D.: The Mid-Pliocene sea-level conundrum: Glacial isostasy, eustasy and dynamic topography, Earth Planet. Sc. Lett., 387, 27–33, 2014.

Salabarnada, A., Escutia, C., Röhl, U., Nelson, C. H., McKay, R., Jiménez-Espejo, F. J., Bijl, P. K., Hartman, J. D., Strother, S. L., Salzmann, U., Evangelinos, D., López-Quirós, A., Flores, J. A., Sangiorgi, F., Ikehara, M., and Brinkhuis, H.: Paleoceanography and ice sheet variability offshore Wilkes Land, Antarctica – Part 1: Insights from late Oligocene astronomically paced contourite sedimentation, Clim. Past, 14, 991–1014, https://doi.org/10.5194/cp-14-991-2018, 2018.

Sangiorgi, F., Bijl, P.K., Passchier, S., Salzmann, U., Schouten, S., McKay, R., Cody, R. D., Pross, J., Van De Flierdt, T., Bohaty, S. M., Levy, R., Williams, T., Escutia, C., and Brinkhuis, H.: Southern Ocean warming and Wilkes Land ice sheet retreat during the mid-Miocene, Nat. Commun., 9, 317, https://doi.org/10.1038/s41467-017-02609-7, 2018.

Scher, H. D. and Martin, E. M.: Circulation in the Southern Ocean during the Paleogene inferred from neodymium isotopes, Earth Planet. Sc. Lett., 228, 391–405, 2004.

Scher, H. D., Whittaker, J. M., Williams, S. E., Latimer, J. C., Kordesch, W. E. C., and Delaney, M. L.: Onset of Antarctic Circumpolar Current 30 million years ago as Tasmanian Gateway aligned with westerlies, Nature, 523, 580–583, 2015.

Seton, M., Müller, R. D., Zahirovic, S., Gaina, C., Torsvik, T., Shephard, G., Talsma, A., Gurnis, M., Turner, M., Maus, S., and Chandler, M.: Global continental and ocean basin reconstructions since 200 Ma, Earth-Sci. Rev., 113, 212–270, 2012.

Shepherd, A., Ivins, E. R., Geruo, A., Barletta, V. R., Bentley, M. J., Bettadpur, S., Briggs, K. H., Bromwich, D. H., Forsberg, R., Galin, N., Horwath, M., Jacobs, S., Joughin, I., King, M. A., Lenaerts, J. T. M., Li, J., Ligtenberg, S. R. M., Luckman, A., Luthcke, S.B., McMillan, M., Meister, R., Milne, G., Mouginot, J., Muir, A., Nicolas, J. P., Paden, J., Payne, A. J., Pritchard, H., Rignot, E., Rott, H., Sørensen, L. S., Scambos, T. A., Scheuchl, B., Schrama, E. J. O., Smith, B., Sundal, A. V., Van Angelen, J. H., Van De Berg, W. J., Van Den Broeke, M. R., Vaughan, D. G., Velicogna, I., Wahr, J., Whitehouse, P. L., Wingham, D. J., Yi, D., Young, D., and Zwally, H. J.: A reconciled estimate of ice-sheet mass balance, Science, 338, 1183–1189, 2012.

Sluijs, A., Brinkhuis, H., Stickley, C. E., Warnaar, J., Williams, G. L., and Fuller, M.: Dinoflagellate cysts from the Eocene – Oligocene transition in the Southern Ocean: Results from ODP Leg 189, in: Proceedings of the Ocean Drilling Program, Scientific Results, edited by: Exon, N. and Kennett, J. P., U.S. Government Printing Office, College Station, Texas, USA, 189, 2003.

Sluijs, A., Pross, J., and Brinkhuis, H.: From greenhouse to icehouse; organic walled dinoflagellate cysts as paleoenvironmental indicators in the Paleogene, Earth-Sci. Rev., 68, 281–315, 2005.

Stocchi, P., Escutia, C., Houben, A. J. P., Vermeersen, B. L. A., Bijl, P. K., Brinkhuis, H., DeConto, R. M., Galeotti, S., Passchier, S., Pollard, D., Klaus, A., Fehr, A., Williams, T., Bendle, J. A. P., Bohaty, S. M., Carr, S. A., Dunbar, R. B., Flores, J. A., Gonzàlez, J. J., Hayden, T. G., Iwai, M., Jimenez-Espejo, F. J., Katsuki, K., Kong, G. S., McKay, R. M., Nakai, M., Olney, M. P., Pekar, S. F., Pross, J., Riesselman, C., Röhl, U., Sakai, T., Shrivastava, P. K., Stickley, C. E., Sugisaki, S., Tauxe, L., Tuo, S., Van De Flierdt, T., Welsh, K., and Yamane, M.: Relative sea-level rise around East Antarctica during Oligocene glaciation, Nat. Geosci., 6, 380–384, https://doi.org/10.1038/ngeo1783, 2013.

Storkey, C. A.: Distribution of marine palynomorphs in surface sediments, Prydz Bay, Antarctica, MSc thesis Victoria University of Wellington, New Zealand, available at: http://hdl.handle.net/10063/21 (last access: July 2018), 2006.

Strother, S. L., Salzmann, U., Sangiorgi, F., Bijl, P. K., Pross, J., Escutia, C., Salabarnada, A., Pound, M. J., Voss, J., and Woodward, J.: A new quantitative approach to identify reworking in Eocene to Miocene pollen records from offshore Antarctica using red fluorescence and digital imaging, Biogeosciences, 14, 2089–2100, https://doi.org/10.5194/bg-14-2089-2017, 2017.

Tauxe, L., Stickley, C. E., Sugisaki, S., Bijl, P. K., Bohaty, S., Brinkhuis, H., Escutia, C., Flores, J. A., Iwai, M., Jimenez-Espejo, F., McKay, R., Passchier, S., Pross, J., Riesselman, C., Röhl, U., Sangiorgi, F., Welsh, K., Klaus, A., Bendle, J. A. P., Dunbar, R., Gonzalez, J., Olney, M. P., Pekar, S. F., and van de Flierdt, T.: Chronostratigraphic framework for the IODP Expedi-

tion 318 cores from the Wilkes Land Margin: constraints for paleoceanographic reconstruction, Paleoceanography, 27, PA2214, https://doi.org/10.1029/2012PA002308, 2012.

Torsvik, T. H., Van der Voo, R., Preeden, U., Niocaill, C. M., Steinberger, B., Doubrovine, P. V., van Hinsbergen, D. J. J., Domeier, M., Gaina, C., Tohver, E., Meert, J. G., McCausland, P. J., and Cocks, L. R. M.: Phanerozoic polar wander, palaeogeography and dynamics, Earth-Sci. Rev., 114, 325–368, 2012.

Van Hinsbergen, D. J. J., De Groot, L. V., Van Schaik, S. J., Spakman, W., Bijl, P. K., Sluijs, A., Langereis, C. G., and Brinkhuis, H.: A paleolatitude calculator for paleoclimate studies, PLoS ONE, 10, e0126946, https://doi.org/10.1371/journal.pone.0126946, 2015.

Wilson, G. S., Bohaty, S. M., Fielding, C. R., Florindo, F., Hannah, M. J., Hardwood, D. M., Mcintosh, W. C., Naish, T. R., Roberts, A. P., Sagnotti, L., Scherer, R. P., Strong, C. P., Verosub, K. L., Villa, G., Webb, P., and Woolfe, K. J.: Chronostratigraphy of CRP-2/2A, Victoria Land Basin, Antarctica, Terra Antarctica, 7, 647–654, 2000.

Wise, S. W. and Schlich, R.: Proceedings of the Ocean Drilling Program, Scientific Results, U.S. Government Printing Office, College Station, Texas, 120, 1992.

Wouters, B., Martin-Español, A., Helm, V., Flament, T., van Wessem, J. M., Ligtenberg, S. R. M., van den Broeke, M. R., and Bamber, J. L.: Dynamic thinning of glaciers on the Southern Antarctic Peninsula, Science, 348, 899–903, 2015.

Wrenn, J. H. and Hart, G. F.: Paleogene dinoflagellate cyst biostratigraphy of Seymour Island, Antarctica, Geological Society of America Memoires, 169, 321–447, 1988.

Xiao, W., Esper, O., and Gersonde, R.: Last Glacial-Holocene climate variability in the Atlantic sector of the Southern Ocean, Quaternary Sci. Rev., 135, 115–137, 2016.

Zachos, J. C., Dickens, G. R., and Zeebe, R. E.: An early Cenozoic perspective on greenhouse warming and carbon-cycle dynamics, Nature, 451, 279–283, 2008.

Zevenboom, D.: Dinoflagellate cysts from the Mediterranean late Oligocene and Miocene, PhD thesis Utrecht University, Utrecht, the Netherlands, 1995.

Zonneveld, K. A. F., Marret, F., Versteegh, G. J. M., Bogus, K., Bonnet, S., Bouimetarhan, I., Crouch, E., de Vernal, A., Elshanawany, R., Edwards, L., Esper, O., Forke, S., Grøsfjeld, K., Henry, M., Holzwarth, U., Kielt, J., Kim, S., Ladouceur, S., Ledu, D., Chen, L., Limoges, A., Londeix, L., Lu, S., Mahmoud, M. S., Marino, G., Matsouka, K., Matthiessen, J., Mildenhall, D. C., Mudie, P., Neil, H.L., Pospelova, V., Qi, Y., Radi, T., Richerol, T., Rochon, A., Sangiorgi, F., Solignac, S., Turon, J., Verleye, T., Wang, Y., Wang, Z., and Young, M.: Atlas of modern dinoflagellate cyst distribution based on 2405 data points, Rev. Palaeobot. Palyno., 191, 1–197, 2013.